Sādhanā (2020)45:278
https://doi.org/10.1007/s12046-020-01514-y

Mechanical, thermal, and water absorption behaviour of jute/carbon reinforced hybrid composites

MARGABANDU SATHIYAMOORTHY and SUBRAMANIAM SENTHILKUMAR*

School of Mechanical Engineering, Vellore Institute of Technology, Vellore 632014, India
e-mail: rmsathyam@gmail.com; ssenthilkumar@vit.ac.in

MS received 25 February 2020; revised 20 July 2020; accepted 11 October 2020

Abstract. The demand for fiber-reinforced composite materials is increasing in structural applications due to their crucial characteristics such as stiffness, strength, and durability and processing benefits at low cost. In this study, jute/carbon hybrid composite laminates were investigated for the effect of fabric hybridization and stacking sequence on tensile, impact, microhardness, water absorption, and thermal behavior of the material. The hand layup process was used to fabricate the composite laminates with four different stacking sequences. The X-ray diffraction (XRD), Fourier-Transform Infrared spectroscopy (FT-IR), Thermogravimetric analysis (TGA), and Scanning Electron Microscope (SEM) were used to characterize the structural morphology and thermal stability of the fabricated composites. The experimental results exposed that the hybridization process enhanced the properties of jute reinforced composites. FT-IR and XRD analysis revealed that the alkalization process removed the binding constituents like lignin and hemicelluloses from raw jute fiber, which resulted in a higher crystallinity index. The TGA analysis proved that the hybrid composites are thermally stable at a higher temperature. The hybrid composite with Jute/Carbon/Carbon/Jute stacking patterns has the highest tensile strength of 234.68 MPa compred to other stacking sequences. The hybrid composite with Carbon/Jute/Jute/Carbon fabric stacking sequence exhibited enhanced impact strength of 108.45 kJ/m^2 and better moisture resistance. The incorporation of jute with carbon declined the tensile strength and impact strength by 22% and 14%, respectively, compared to carbon-reinforced composites. The surface micrographs of the fractured samples exhibit the interfacial bonding of fiber/matrix, matrix crack, fiber fracture, and fiber pullouts.

Keywords. Hybrid polymer composite; stacking sequence; mechanical properties; thermal behaviour; water absorption.

1. Introduction

The demand for fiber-reinforced composite materials in structural applications is increasing from the past several years, owing to its superior strength, less weight, toughness, wear resistance, and more processing benefits at low cost [1, 2]. The reinforcement fibers are categorized into synthetic (manmade) fibers and natural bio-fibers. Manmade inorganic fibers, namely aramid, carbon, and E-glass are widely used in aeronautical, marine, and defense applications where high cost is not of more significance [3]. However, the composites reinforced with synthetic fibers are facing specific issues at the end of its lifespan, since it is non-ecofriendly and non-biodegradable [4, 5]. Recently, researchers are focusing their interest to overcome the drawbacks by investigating biodegradable fibers, such as bamboo, bagasse, flax, jute, and coir to minimize environmental problems. The utilization of bio-fibers as alternate reinforcements for manmade fibers in composites is increasing due to their advantages, such as abundant availability, less price, low density, high stiffness, non-toxic, eco-friendly, and renewability [6]. Besides the ecological benefits, natural fibers offer lower density compared with glass fiber and better damping performance compared with carbon fiber [7].

Amongst natural fibers, jute fibers are receiving higher acceptance due to its better stiffness, since it has high cellulose content compared to other natural fibers. Furthermore, jute has less density and minimizes the mass of the composites to a greater extent, in that way the composites developed with jute fiber are more economic [8]. The natural fibers exhibit limitations like low impact resistance, higher sensitivity to water absorption owing to its hydrophilic character, poor thermal stability, and poor interface adhesion between fiber-matrix [9], which degrade the mechanical performances of the composites. Consequently, combining the synthetic and natural fibers (Hybridization) in a single matrix offers a good balance of mechanical performance and cost of the fibers [10–12]. Incidentally, the research was motivated to examine the

*For correspondence
Published online: 06 November 2020

mechanical properties of hybrid jute/glass and jute/carbon composites.

Ahmed *et al* [13] examined the effect of fabric arrangements on the mechanical behaviour of hybrid jute/glass composites and found that the incorporation of glass fiber to jute enhanced the mechanical properties of jute composites. Flynn *et al* [14] examined the mechanical properties of hybrid flax-carbon composites and concluded that hybridized flax/carbon composites showed higher mechanical strength. Gujjala *et al* [15] found the influence of stacking order on the mechanical performances of hybrid jute/glass composites and concluded that the tensile and interlaminar shear strength was maximum for the laminates (GJJG) having stacking order of Glass-Jute-Jute-Glass, and the flexural strength was higher for the laminate with "GJGJ" layering pattern. Rafiquzzaman *et al* [16] investigated the mechanical properties of glass-jute hybrid composites using experimental and numerical methods and found that the incorporation of the optimal quantity of jute with glass fiber increased the overall properties with cost-effectiveness. Abdelbaky [17] investigated the tensile and bending performances of hybrid jute-glass-carbon epoxy composites with different layer configurations. The authors reported that the layering patterns of composites do not have an impact on tensile properties; whereas, the composite which has carbon as external layers exhibited peak flexural properties.

Sezgin *et al* [18] developed the jute-glass and jute-carbon polyester laminates to examine the effect of layering order on tensile and impact performances. The hybrid composite with carbon fabric as inner plies had maximum tensile strength and the composite with glass fabric as extreme plies indicated higher impact strength. Nayak *et al* [19] examined the thermal stability of the bamboo/glass composites hybrid composite and found that hybrid composite can withstand at higher degradation temperature than bamboo fiber composites. Jarukumjorn *et al* [20] and Atiqah *et al* [21] observed comparable findings for sisal/glass and sugar palm/glass fiber reinforced composites. Margabandu *et al* [22] examined the effects of layering arrangements on the bending and impact properties of hybrid jute/carbon composites. From the literature, it is found that the fabric arrangements have significant influences on the flexural performances and less effect on the impact strength of the hybrid composites.

The existing literature was mostly concentrated on the impact of the hybridization of different natural fibers with synthetic glass fiber reinforced composites. However, few studies reported the hybridization of jute/carbon reinforced composites, but the thermal behaviour of hybrid jute-carbon composites was not analyzed adequately. In the present study, jute and carbon fabrics are used as reinforcements in the epoxy matrix to develop hybrid composites with different stacking sequences to examine the influence of hybridization on thermal stability, moisture uptake, tensile, and impact properties of jute/carbon hybrid composites. The effect of fabric arrangements on the mechanical properties of hybrid composites is also studied. Characterization studies, such as X-ray diffraction, Fourier transform infrared spectroscopy, thermogravimetric analysis, and scanning electron microscopy were carried out to analyze the modifications in the crystallinity index, chemical compositions, thermal stability, and morphology of the composite specimens. For better understanding, the characterization studies for the untreated jute fiber was performed and compared with alkali-treated jute fiber.

2. Experimental work

2.1 *Materials*

The plain-woven jute fabric and 2 × 2 twill weave carbon fabrics are used as reinforcing materials. The matrix system contains "Araldite LY556"-epoxy resin and "Aradur HY951" hardener. The areal density of jute fiber and carbon fiber is 264 g/m^2 and 300 g/m^2. The mechanical properties of jute fabrics, carbon fabrics, epoxy, and hardener are given in tables 1 and table 2, correspondingly.

2.2 *Alkali Treatment of Jute Fiber*

Naturally, the hydrophilic character of natural fibers tends to absorb more quantity of moisture, which often causes incompatible with the polymer matrix [24]. The natural fibers are exposed to different treatments, such as alkali treatment, acetylation, enzyme, methacrylate, and sodium chlorite, which results in improved mechanical properties and enhanced adhesion between fiber and matrices [25, 26]. Among different methods, alkalization is an effective process to improve the fiber-matrix interaction, thermal stability, and heat resistance [27, 28]. A study [29] on alkali treatment of jute fabrics with different concentrations (1, 5, and 17.5 wt%) of sodium hydroxide (NaOH) solution revealed that 5% NaOH treatment is the optimum concentration for the jute fabrics. In the present work, all the jute fabrics were pretreated using a 5% NaOH solution before the fabrication of composite laminates. NaOH alkaline solution was prepared by dissolving 250 g of NaOH pellets in 5 liters of de-ionized water in a tray. Earlier, the jute fabrics were rinsed in normal water for the

Table 1. Properties of jute and carbon fabrics.

Mechanical properties		
Properties	Jute fabric [23]	Carbon fabric
Density (g/cm^3)	1.3–1.5	1.8
Tensile strength (MPa)	393–800	3500–5000
Young's modulus (GPa)	10–55	260
Elongation at break (%)	1.5–1.8	1.4–1.8

Table 2. Properties of epoxy and hardener.

Properties	LY556-Epoxy resin	HY951-Hardener
Appearance	Clear liquid	–
Viscosity at 25°C (mPa s)	10,000–12,000	10–20
Density at 25°C (g/cc)	1.15–1.20	0.97–0.99
Flash point (°C)	>200	>180

Table 3. Laminate codes.

Sample group	Fabric arrangements/sequences
S1	Jute-Jute-Jute-Jute
S2	Carbon-Carbon-Carbon-Carbon
S3	Jute-Carbon-Carbon-Jute
S4	Carbon-Jute-Jute-Carbon

removal of impurities and other unwanted constituents. The fabrics are dried for 48 hours at ambient temperature. The moisture-free fabrics were immersed in 5 wt% NaOH solution for about 2 hours and washed three times in running water to eliminate any observed NaOH content remains in it and dried out in an oven at 60°C for about 4 hours followed by drying at an ambient temperature of about 24 hours [30]. All the alkali-treated jute fabrics were ironed by the manual iron box to remove shrinkages and also to get the proper arrangement of fibers since it was misaligned during mercerization [31].

2.3 *Composite Laminate Preparation*

Four groups of composite laminates with different sequencing orders are fabricated by using a simple hand-layup method at an ambient temperature of about 23±2°C on the tile slab. table 3 lists the fabric arrangements and laminate codes. Figure 1 represents the fabric arrangements of composite laminates. Fabrics of jute and carbon were cut into 300 × 300 mm^2 and utilized for the experiments. During the fabrication process, four plies were maintained with 0°/90° fabric orientation in all the composite laminate samples.

The jute plies were placed in an oven for about 12 hours at 70°C to remove the humidity content [32] before the fabrication process. During fabrication, the epoxy and hardener were blended with the proportion of 10:1 by stirrer rod for 10 minutes to obtain bubbles free homogenous mixture. This mixture was applied uniformly by brush on the tile slab, followed by stacking the first fabric layer over it. In the same method, the remaining three fabric layers were laid one over the other. On top of all, a tile slab was kept and the deadweight of 35 kg was placed over it to achieve flatness and uniform thickness of the composite. The entire set-up was allowed for curing at 25°C for about 24 hours, subsequently, the deadweight was removed and the prepared composites are placed in an industrial oven at 50°C for 3 hours for post-curing [33, 34]. The cured composites were cut into appropriate dimensions as per ASTM standards to perform characterization and mechanical tests.

3. Characterizations

3.1 *Mechanical Testing*

The tensile behaviour of the composite samples was determined as per the ASTM D3039 standard using Instron 8801 universal testing machine. The dimensions of the test samples were 300 × 25 × 4 mm^3. The Charpy impact test on specimens was conducted based on ASTM standard D6110 by using Tinius Olsen digital pendulum impact testing machine. The dimensions of test specimens were 127 × 12.7 × 4 mm^3. Five identical samples from the individual category were tested, and the average result was considered.

3.2 *Microhardness test*

The micro indentation was carried out based on the ASTM E384 standard using the Matsuzawa microhardness tester. Initially, the prepared samples were cleaned and polished by using a double disc polishing machine. The microhardness value of the polished samples was found by

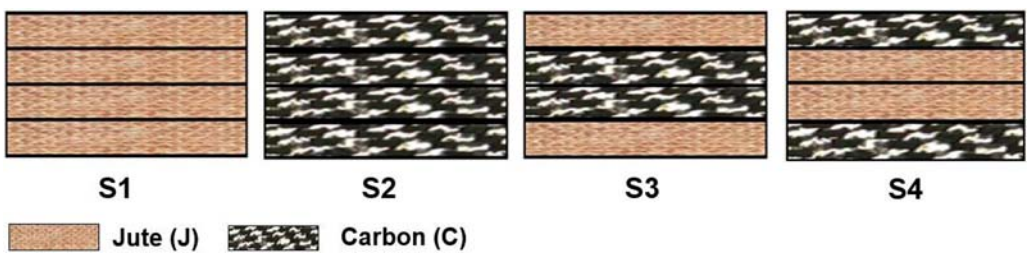

Figure 1. Fabric arrangements of composite laminates.

Vickers pyramid diamond indenter having an included angle of 136°, under the load of 100 gf and a dwell time of 10 seconds. The indentations were done at ten different points on the individual specimen, and the average was noted.

3.3 *X-Ray Diffraction (XRD) Analysis*

The X-ray diffraction analysis of composite samples has been conducted using Bruker D8 advanced diffractometer, equipped with Cu, Kα radiation (λ = 1.5406 Å) at an operating condition of 40 kV and 30 mA. The crystallinity index (CI) and crystallinity percentage of the fibers are calculated by using equations 1 and 2 [35].

$$\text{Crystallinity Index (CI)} = \left(S_c - S_a/S_c\right) \quad (1)$$

$$\text{Percentage of crystallinity } (\%) = \left(S_c/S_c + S_a\right) \times 100 \quad (2)$$

where S_c and S_a are the maximum intensity of the crystal plane and amorphous phase, respectively.

3.4 *Fourier-Transform Infrared Spectroscopy (FTIR)*

The infra-red spectrum of the composite specimens was characterized using the Shimadzu FTIR spectrometer. The spectrums were recorded in the transmittance range of 400 to 4000 cm^{-1} with a resolution of 4 cm^{-1} using the potassium bromide (KBr) disk method.

3.5 *Thermogravimetric Analysis (TGA)*

The thermogravimetric analysis of jute/carbon composite samples was performed using (Make: TA Instruments, USA) SDT Q600 Model analyzer. All measurements were made from 20°C to 800°C at a constant 20°C/min in a nitrogen environment. The mass of all the samples is maintained at a range of 5–6 mg.

3.6 *Moisture Absorption*

The moisture absorption behaviour of prepared specimens was investigated based on ASTM D-5229 standard to predict the stability of prepared composites under a moisture environment. Four samples with dimensions of 100 × 100 × 4 mm^3 and the edges were sealed by epoxy resin to avoid the water intake at the edges. Before the test, all the samples were kept in an industrial oven for about 24 hours at 70°C and noted the mass of specimens as baseline mass (w_b). The samples were immersed in distilled water for 65 days at 25°C. The immersed samples were withdrawn from water and weighed regularly to determine the weight change. The percentage of moisture absorption was calculated by equation (3).

$$\text{Moisture absorption content, } M_t(\%) = \left(m_t - m_o/m_o\right) \times 100 \quad (3)$$

where m_t is the mass of the wet sample at a specific time t during immersion and m_o is the mass of the dry sample at the initial time.

3.7 *Scanning Electron Microscope (SEM)*

The micrographs for the fractured specimens were analyzed with SEM (Carl Zeiss EVO18) at 10 kV acceleration voltage. Ahead of the morphology investigation, the specimens were sputter-coated with gold particles in an ionizer to enhance the electrical conductivity.

4. Results and discussion

4.1 *Tensile Strength*

The tensile behaviour of the composite laminate depends on fiber strength and modulus, interfacial bonding of fiber with matrix, types of weaving patterns, and the fabric arrangements. Figure 2 illustrates the tensile strength of composites containing the equal number of fabric layers with different arrangements. The tensile strength of jute fiber composite (S1) is found to be 54.98 MPa. Pure carbon fiber-reinforced composite (S2) exhibited maximum tensile strength than the other composites since the tensile strength of carbon fiber is greater than jute fiber. The hybrid composites possess a higher tensile strength than the pure jute composite. The improvement in the tensile strength of the

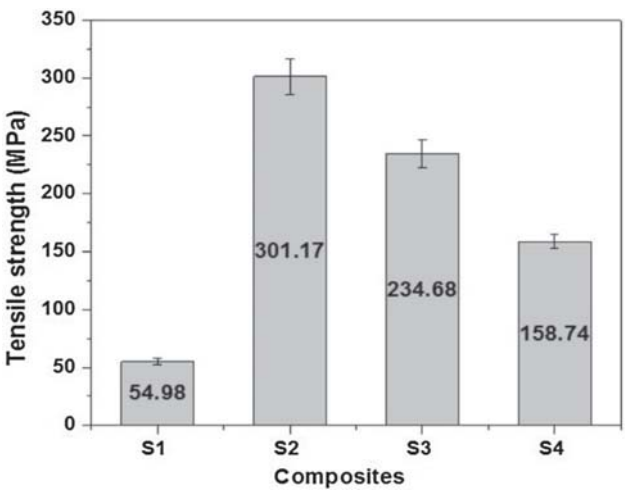

Figure 2. Tensile strength of hybrid jute/carbon composites.

composites is due to the incorporation of carbon fiber with jute. Moreover, it is observed that replacing two layers of carbon fibers with two layers of jute in hybrid composite (S3), reduced the tensile strength only by 22%. It is due to the fabric arrangements of carbon at the middle and jute at surface sides, and the strong interfacial bonding of fibers with epoxy, which is confirmed by SEM morphology. In hybrid composite (S4), the reduction in tensile strength compared with S2 is 47%. The results have revealed that the tensile strength of the composites is not only influenced by fabric hybridization. It also depends on the arrangements of the fabrics in the composites, which is also evidenced by the previous study carried out by Gujjala *et al* [15] for hybrid jute/glass composites. The arrangement of high strength fabrics at middle and low strength fabrics at outer surfaces resulted in enhanced tensile strength.

4.2 *Impact Strength*

The impact toughness of hybrid jute/carbon reinforced composites is shown in figure 3. The composite (S1), reinforced only with jute fiber showed the impact strength of 40.71 kJ/m^2. The pure carbon composite (S2) offers maximum impact strength, which is greater than all the composites. The impact strength of hybrid composite S3 was enhanced by 65% of S2 composite. Compared to S3 composites, S4 composites show a 32% higher impact strength. The hybrid composite (S4), declined the impact strength only by 14% compared to the S2 composite. It is visible that the addition of carbon fibers to the jute fibers enhanced the impact toughness of the hybrid composites. Moreover, it is observed that the stacking sequences have a noticeable influence on the impact properties of hybrid composites. The enhancement in the impact toughness of composite S4 is due to moderate bonding of fiber and matrix, which is essential to absorb higher impact energy [36, 37]. It is supported by morphology analysis. Naveen *et al* [38] noticed a similar kind of behaviour for hybrid Kevlar/Cocos sheath composites.

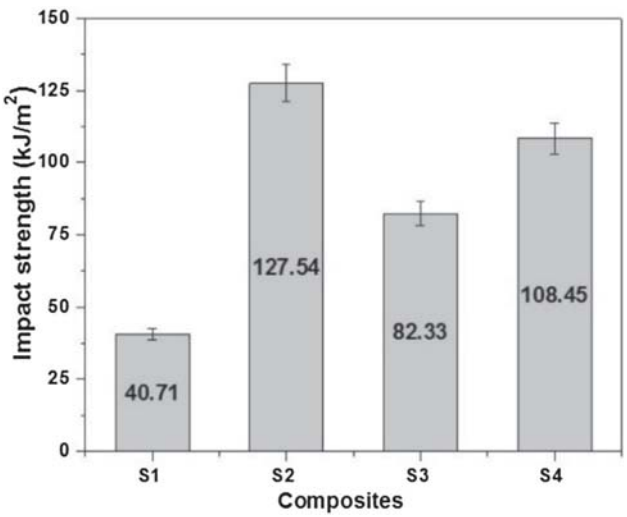

Figure 3. Impact strength of hybrid jute/carbon composites.

Table 4. gives the earlier work reported on the mechanical properties of single and hybrid fiber-reinforced polymer composites. From the table, it is evident that the developed hybrid jute/carbon epoxy composites(S4) demonstrated better mechanical properties.

4.3 *Microhardness*

The microhardness of the jute/carbon hybrid composites is represented in figure 4. The composite (S1) has the lowest hardness than the other composites due to the poor mechanical strength of jute fiber than carbon fiber and improper adhesion between jute with epoxy. Pure carbon composite (S2) showed the maximum hardness among all the composites due to strong adhesion between the carbon fiber with polymers. The hybrid composites S3 and S4 showed higher hardness than the composite S1. The results revealed that the incorporation of high strength carbon fiber enhanced the hardness of hybrid composites. Among hybrid composites, the composite laminate S4 showed a 19% higher hardness than S3 composites. The improvement in hardness of hybrid composite S4 is due to the stacking of jute and carbon fibers in different orders. Furthermore, the high strength carbon fibers (positioned at surface sides) reduced the penetration of diamond intenders into the surface of S4 composites. It is noticeable that the sequencing order of fabrics has considerable influences on the hardness of hybrid composites.

4.4 *X-ray Diffraction*

XRD pattern with diffraction peaks of fiber composite samples is depicted in figure 5. The significant intensity peaks for the raw jute and treated jute fiber composites at $2\theta = 17°$ and 23° indicate the presence of cellulose I [46]. It is noted from the plot that the alkali treatment performed in this study, is not altered the fiber cellulose structure. Table 5 lists the determined crystallinity index and percentage of the untreated jute fiber, treated jute fiber (S1), and hybrid fibers (S4) samples. The crystallinity index of raw fiber and treated fibers are 68.65% and 71.22% respectively, which indicates that the chemically treated jute fiber possesses more degree of crystallinity compared with untreated fibers. The enhancement in the crystallinity is ascribed to the elimination of lignin and hemicelluloses after alkalization [35]. The diffraction peaks of hybrid composites are exhibiting at 18.30° (epoxy phase), 34.17°, 35.82°, 38.34°, 41.40°, 59.88°, and 71.98°. This increment in the number of crystalline peaks is due to the effective hybridization of both fibers in epoxy composites. In

Table 4. Work reported on the mechanical properties of fiber-reinforced polymer composites.

Single fiber reinforced polymer composites				
Fiber material	Matrix material	Tensile strength (MPa)	Impact strength	Reference
Jute	Polyester	30.59	18.95 (Kj/m2)	[18]
Jute	Epoxy	50.64	1.3 (J)	[39]
Jute (S1)	Epoxy	54.94	40.17 (Kj/m2)	Current study
Carbon	Polyester	291.82	121.03 (Kj/m2)	[18]
Carbon	Epoxy	288.03	4.58 (J)	[40]
Carbon	Epoxy	210.7	230.8 (J/m2)	[41]
Carbon (S2)	Epoxy	301.17	127.54 (Kj/m2)	Current study
Hybrid fiber reinforced polymer composites				
Sisal/Glass/Banana	Epoxy	104	12.8 (J)	[42]
Flax/Carbon	Epoxy	126.30	–	[43]
Abaca/Glass	Epoxy	44.5	16 (J)	[44]
Cocus sheath/Kevlar	Epoxy	51.67	76.89 (Kj/m2)	[38]
Sisal/Glass/Chitosan	Epoxy	135	–	[45]
Jute/Glass	Epoxy	56.68	5.49 (J)	[6]
Jute/Carbon	Epoxy	102.87	104.79 (Kj/m2)	[18]
Jute/Carbon (S4)	Epoxy	158.74	108.45 (Kj/m2)	Current study

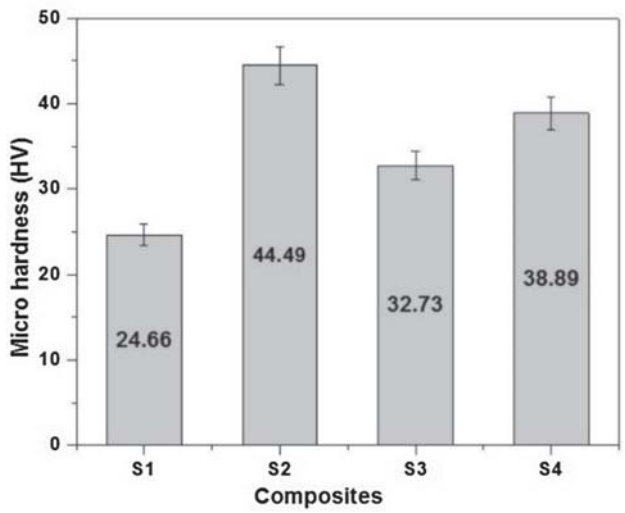

Figure 4. Microhardness of the hybrid jute/carbon laminates.

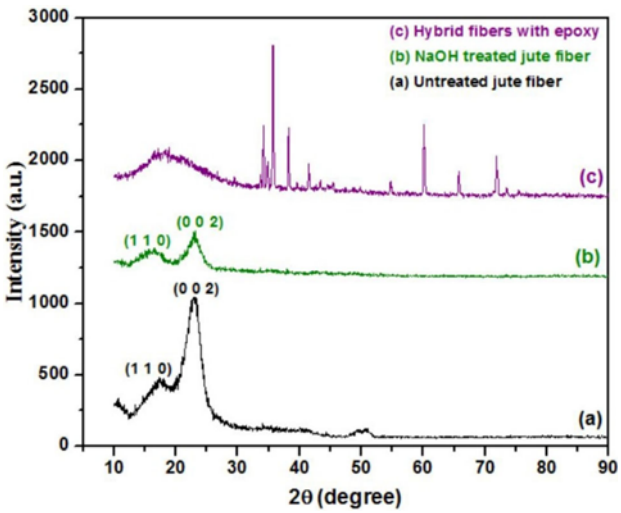

Figure 5. XRD pattern of fiber samples.

general, the increment in the crystallinity of the composite enhances its hardness and other mechanical properties [47]. The present work confirms that hybrid composites show enhancement in both tensile and impact strength due to the addition of carbon fibers.

4.5 *FTIR Spectroscopy*

The FTIR spectroscopy is used to identify the functional groups existing in the prepared composites. table 6 summarizes the chemical compositions of the reinforced fibers and the corresponding position of peaks for the untreated jute, treated jute (S1), and hybrid composites (S4). The dominant broadband at 3380.40 cm^{-1} is related to the O-H stretching of hydroxyl groups. The broadness of the band decreases due to the removal of hydrogen bonds upon alkalization with NaOH. The peak located at 2919.67 cm^{-1} is assigned to C-H stretching. The band 1730.56 cm^{-1} is related to C-O stretching in a carboxylic group of hemicellulose in jute fiber. The peak disappeared after the treatment, which is represented in table 6, due to the elimination of hemicelluloses by the alkali process. The peak observed at 1646.58 cm^{-1} in untreated jute is ascribed to C-C stretching, which is reduced to 1606.06 cm^{-1} for the

Table 5. Crystallinity percentage and crystallinity index of hybrid jute/carbon composites.

Sample type	Maximum intensity of the crystal plane (I_{002})	Peak position (2θ)	Maximum intensity of amorphous phase (I_{002})	Peak position (2θ)	Crystallinity index (CrI)	Crystallinity percentage (%)
Untreated jute	991.21	23.08	448.42	17.27	0.55	68.85
Treated jute (S1)	334.65	22.90	135.23	16.17	0.60	71.22
Jute with carbon (S4)	1087.90	35.61	386.54	18.03	0.64	73.78

Table 6. Peak assignment of FTIR spectra for the prepared composites.

Assignments	Wavenumber (cm^{-1})			Reference
	Untreated jute sample	Treated jute sample (S1)	Hybrid sample (S4)	
O-H stretching (hydrogen bond)	3380.40	3330.04	3340.61	[48]
C-H stretching vibration of methyl and methylene	2919.67	2919.09	2926.09	[49]
C-O stretching in carbonyl and unconjugated β-ketone	1730.56	Nil	Nil	[50]
C=C stretching vibration	1646.58	Nil	1606.06	[51]
C-H deformation and CH_2 bending	1422.44	1420.50	1456.26	[52]
C-O stretching in acetyl group	1239.85	Nil	1232.36	[53]
C-H stretching vibration	1030.80	1027.36	1031.31	[53]
C-H out of plane vibration	853.77	Nil	826.34	[53]
C-OH bending vibration	556.94	545.55	554.27	[23]

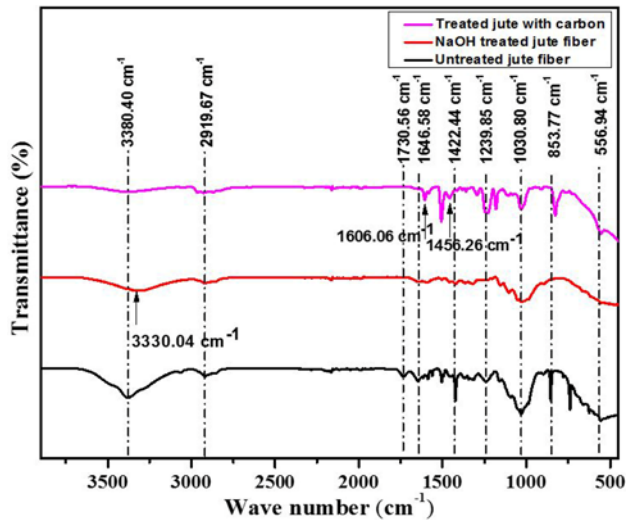

Figure 6. FTIR spectra of hybrid jute/carbon fibers.

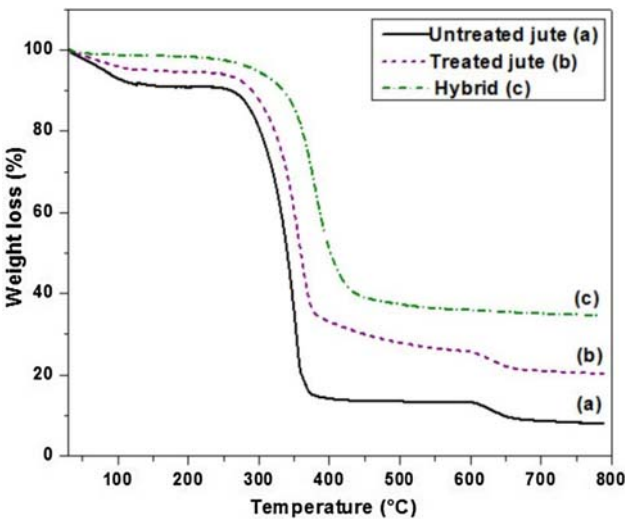

Figure 7. TGA analysis of jute/carbon composites.

treated jute fiber, since the oil and impurities are eliminated from raw jute fiber surfaces. The peak at 1422.44 cm^{-1} is related to the CH_2 degradation in lignin. The increased intensity peaks at 1456.26 cm^{-1}, corresponding to increases in cellulose content due to the absence of other fiber constituents. The band at 1239.85 cm^{-1} and 1232.36 cm^{-1} is attributed to C-O stretching in the acetyl group of untreated and treated fiber. The peak observed at 1030.80 cm^{-1}, 853.77 cm^{-1}, and 556.94 cm^{-1} are related to the stretching mode of C-H, out of plane vibration mode of

Table 7. Stages of thermal degradation and weight loss of the composites.

Composite samples	Major degradation temperature (°C)	Weight loss (%)	Final degradation temperature (°C)	Residue (%)
Untreated jute fiber	153	74.63	390	7.88
Treated jute fiber (S1)	161	66.68	401	20.22
Hybrid composites (S4)	165	60.98	451	34.55

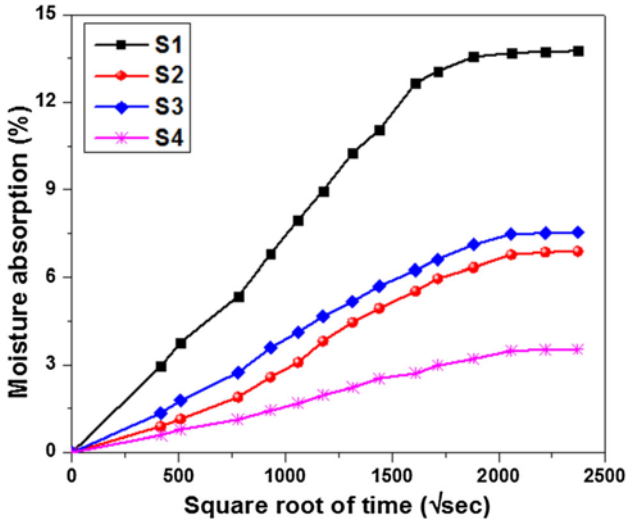

Figure 8. Moisture absorption behaviour of hybrid jute/carbon composites.

C-H, and bending mode of C-OH. It is observable that untreated fibers have a higher intensity band compared to treated jute fibers. Furthermore, all the obtained peaks of hybrid samples (jute with carbon) show the noticeable structural changes as compared with other composite specimens. Figure 6 depicts the FTIR spectrum of the hybrid jute/carbon fiber composites.

4.6 *Thermogravimetric Analysis (TGA)*

Thermogravimetric analysis was carried out to examine the thermal stability and weight loss of polymer composites exposed to higher temperatures. Figure 7 depicts the TGA curve of untreated jute, treated jute, and hybrid composite samples. The degradation temperature of all the samples exhibited within the range of 30°C to 500°C. In general, surface treated fibers shows higher thermal stability than untreated fiber [54]. The mass loss of the composite samples occurred in three phases. The initial phase of weight loss was noticed at the temperature range from 30°C to126°C, corresponding to the loss of moisture content. The second phase of mass loss occurred at a temperature range between 153°C to 306°C, corresponding to the decomposition of lignin and hemicelluloses components. The final phase of mass loss occurred with the temperature range of 306°C to 390°C as a consequence of cellulose degradation. Kabir *et al* [55] observed a similar trend and described that the disintegration of lignin, hemicellulose, and cellulose occurred at the temperature range of 25°C to 150°C, 200°C to 380°C, 310°C to 380°C, respectively.

The initial phase (loss of moisture) of all the samples shows a similar trend and decomposition temperature. In the second phase of degradation, the untreated jute fiber decomposed faster than the alkali-treated jute fiber. The surface treatment improves the thermal stability of treated jute fiber resulting in enduring at higher working temperatures. Moreover, it confirms that the improvement in the thermal stability of hybrid composites is due to the incorporation of carbon fiber with jute. Table 7 shows the degradation percentage of the untreated jute, treated jute (S1), and hybrid composites (S4). The percentage of mass loss for the treaded jute fiber and hybrid fibers was less than the untreated fiber. It is evident by the higher decomposition rate of raw jute fiber in lesser temperatures compared to other composites.

4.7 *Moisture Absorption*

The composites reinforced with natural fibers are more sensitive to moisture due to hydrophilic nature. The moisture absorption characteristics of the composites are essential to consider when exposed to a moisture environment. Figure 8 displays the influence of layering order on moisture absorption of hybrid jute/carbon composites. Each curve plotted with the mean value of five samples. The composite-S1 showed the highest moisture absorption of 13.76%, followed by 7.53% (S3), 6.88% (S4), and 3.54% (S2). The obtained result shows that in all the composites, the water intake increased steadily at the initial time of immersion and gets slower and finally reached the equilibrium condition (increase in the mass percentage of the sample is less than 0.01%). The maximum moisture intake of S1 composite is due to more voids and affinity of jute fiber towards moisture. The pure carbon composite S2 offers the least moisture absorption because of its hydrophobic character, and proper adhesion between the carbon with matrix, which reduces the diffusion of water particles. The hybrid composites S3 and S4 show the reduction in moisture uptake of 45% and 50%, respectively, compared to S1 composite. Incorporation of carbon with jute resulted in better moisture resistance. Moreover, the moisture uptake of the hybrid composites is significantly affected by fabric arrangements. The hybrid composite S4

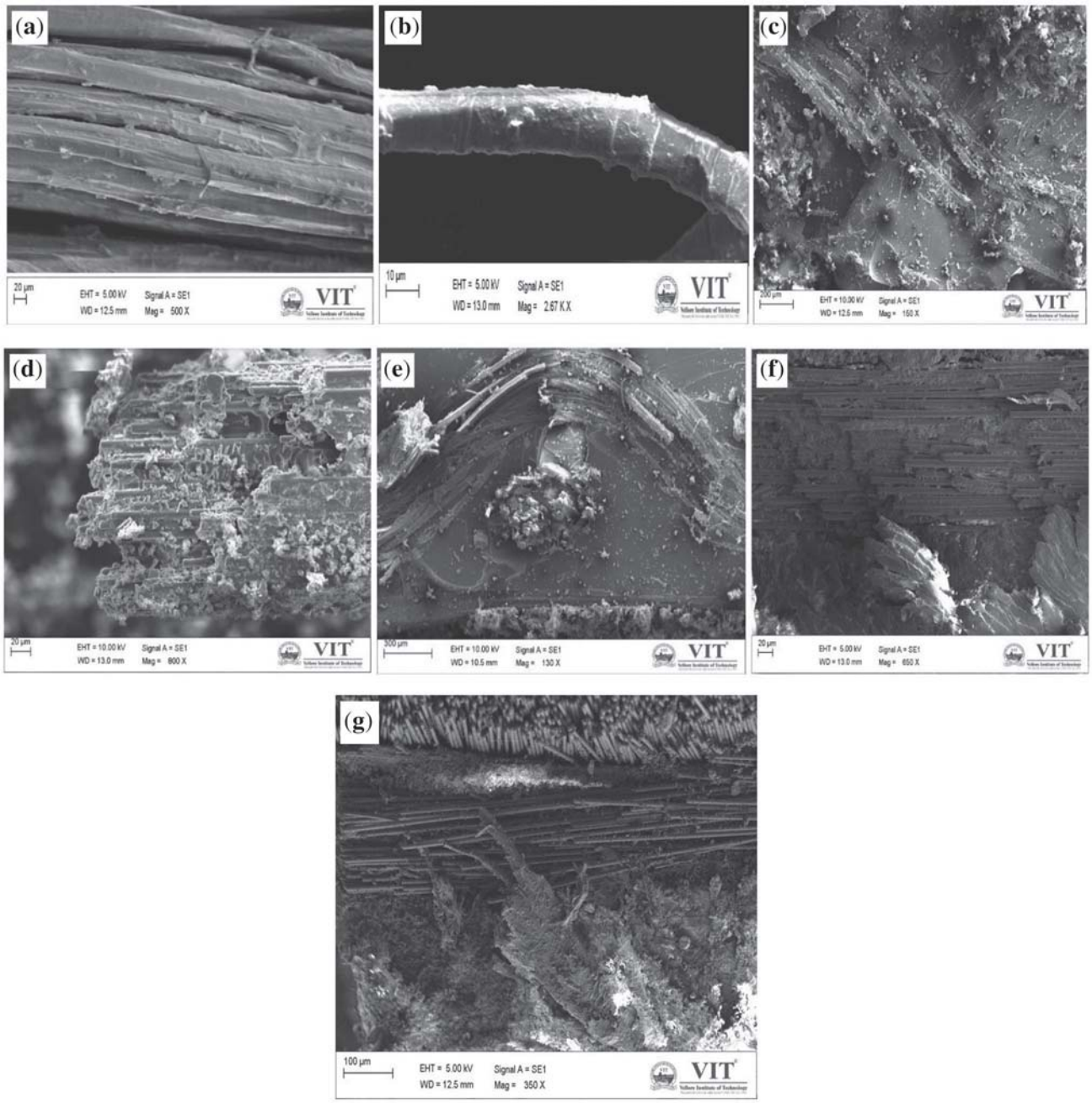

Figure 9. SEM morphology of composite specimens (a) Untreated jute fibers, (b) Treated jute fiber, (c) Pure jute composites-S1, (d) Pure carbon composites-S2, (e) Hybrid composites-S3, (f) Hybrid composites-S4 and (g) Moisture absorbed hybrid sample.

offers the least moisture absorption compared to composite S3, due to the stacking arrangement of carbon fibers to the outer layers. It indicates that the hybrid composite S4 possesses high water resistance since the carbon fabrics at the outer layer prevent the diffusion of water into the composites. The results of moisture absorption behaviour are in closer agreement with the experimental results of earlier work [8].

4.8 *SEM Morphology Analysis*

The SEM micrographs of prepared and fractured composite specimens are represented in figure 9. Morphology of raw jute fiber shows that the presence of wax, lignin, hemicellulose, cellulose, and some other impurities in the form of uplifted filaments on their surfaces, as depicted in figure 9(a). After alkalization, the filaments have

vanished from the treated fiber, and the fiber becomes more visible, as indicated in figure 9(b). Furthermore, it shows that the surface roughness increased due to alkali treatment results in enhancing fiber-matrix bonding. Fiber stretching and fiber breakages are visible in many places of fractured pure jute composites (S1), as represented in figure 9(c). It is attributed to the brittle nature of jute fibers. Further, it shows that jute fiber composites have more matrix crack and void, which affected the mechanical properties of the composite. Figure 9(d) illustrates the micrograph of pure carbon composites (S2), which has fewer fiber pullouts compared to fiber fractures, results in good fiber-matrix adhesion. Figure 9(e) displays the micrographs of fractured hybrid composite S3. The good bonding between the fibers with matrix and fewer fiber pull-outs is visible in the composites resulted in enhanced tensile strength. Figure 9(f) shows that the hybrid composite S4 has more fiber pullouts and moderate interfacial fiber-matrix bonding, which improved the impact energy absorption of the composite. Figure 9(g) shows the water absorbed hybrid composite sample. It is clear that exposure to moisture significantly degrades the fiber-matrix interactions.

5. Conclusion

In the present study, jute/carbon hybrid composite laminates were fabricated and investigated for the influence of fabric incorporation and stacking sequences on thermal stability, moisture absorption, tensile strength, and impact properties. The following conclusions were derived from the experimental investigation.

- Hybridization and stacking sequences of fabrics have a noticeable impact on the mechanical and thermal properties of the hybrid composites.
- XRD analysis confirms the increase in the crystallinity index of 0.64 due to the hybridization of fibers.
- FTIR spectrum revealed that the elimination of lignin and hemicellulose takes place due to mercerization, which resulted in increased cellulose content for treated fiber.
- TGA results exposed that the surface-treated jute composites hold higher degradation temperature compared to untreated jute composites, resulted in improved thermal stability. Moreover, hybrid composites exhibit better thermal stability than other natural composites.
- Investigation on tensile strength revealed that the hybrid composite sequence S3 has declined tensile strength by 22% compared to pure carbon composite S2. Among the other hybrid composite sequences, S3 composite sequence shows 48% higher strength than that of S4, due to the stacking of carbon fabrics as core layers and higher interfacial bonding of fibers with matrix.
- The hybrid composite S4 exhibited the highest impact strength of 108.45 kJ/m^2, which is 14% lesser than the hybrid composite sequence S2. It is due to fewer fiber pullouts and moderate fiber-matrix bonding in S4. On the other hand, stacking the high impact resistance fiber as a skin layer, resulted in higher impact strength.
- The composite laminate sequence S4 exhibit 19% higher hardness than the composite sequence S3, since the carbon fibers at surface sides restricted the penetration of diamond intenders into the S4 composites.
- The incorporation of hydrophobic carbon fiber to the jute composite increases the moisture resistant. The hybrid composite sequence S4 offers better moisture resistance than S3 composite. It is due to the carbon fabrics at the outer layer prevents the diffusion of water into S4 composite sequence.
- The SEM micrograph revealed that NaOH treatment improved the surface roughness of jute fiber. It is due to the elimination of unwanted constituents from the fiber surfaces, that resulted in enhanced interfacial adhesion of fibers with matrix. Besides, the moisture absorption affected the fiber-matrix bonding of the composites.

The study concludes that the hybrid composite sequence S3, with Jute/Carbon/Carbon/Jute stacking order offers high tensile strength and the composite sequence S4 with Carbon/Jute/Jute/Carbon fabric arrangements exhibited better impact strength, better moisture resistance, and higher thermal stability. As a result, the developed lightweight and low-cost hybrid composites would be an appropriate choice for medium load applications, like construction partition boards, door frames, automobile/railway interior panels, suitcases, helmets, etc.

List of symbols

°C	Temperature in Celsius
w_b	Baseline mass of the specimens
M_t	Moisture absorption content
m_t	Mass of the wet sample at a specific time t during immersion
m_o	Mass of the dry sample at the initial time
S_c	Maximum intensity of the crystal plane
S_a	Maximum intensity of the amorphous phase
XRD	X-ray Diffraction
2θ	Peak position
CrI	Crystallinity index
FTIR	Fourier-Transform Infrared Spectroscopy
TGA	Thermogravimetric Analysis
SEM	Scanning Electron Microscope

References

[1] Gay D, Hoa S V and Tsai S W 2003 *Composite materials. Design and applications.* Boca Raton, FL: CRC Press

[2] Jawaid M, Khalil H P S A, Bakar A A and Khanam P N 2011 Chemical resistance, void content and tensile properties of oil palm/jute fiber reinforced polymer hybrid composites. *Mater. Des.* 32: 1014–1019

[3] Kalaprasad G and Thomas S 1995 Hybrid fiber reinforced polymer composites. *Int. Plast. Eng. Technol*. 1: 87–98

[4] Subramonian S, Ali A and Amran M 2016 Effect of fiber loading on the mechanical properties of bagasse fiber-reinforced polypropylene composites. *Adv. Mech. Eng.* 8: 1–5

[5] Howarth J, Mareddy S S and Mativenga P T 2014 Energy intensity and environmental analysis of mechanical recycling of carbon fiber composite. *J. Clea. Prod.* 81: 46–50

[6] Braga R A and Magalhaes Jr P A A 2015 Analysis of the mechanical and thermal properties of jute and glass fiber as reinforcement epoxy hybrid composites. *Mater. Sci. Eng. C*. 56: 269–273

[7] Shamsuyeva M, Hansen O and Endres H 2019 Review on hybrid carbon/flax composites and their properties. *Int. J. Polym. Sci*. https://doi.org/10.1155/2019/9624670

[8] Elbaky M A and Attia M A 2019 Water absorption effect on the in-plane shear properties of jute-glass-carbon reinforced composites using Iosipescu test. *J. Compos. Mater*. 53: 3033–3045

[9] Pandita S D, Yuan X and Manan M A 2014 Evaluation of jute/glass hybrid composite sandwich: Water resistance, impact properties ad life cycle assessment. *J. Reinf. Plast. Compos.* 33: 14–25

[10] Khan M A, Ganster J and Fink H P 2009 Hybrid composites of jute ad man-made cellulose fibers with polypropylene by injection moulding. *Compos. Part A: App. Sci. Manuf.* 40: 846–851

[11] Mohan R and Kishore 1985 Jute-glass sandwich composites. *J. Reinf. Plast. Compos.* 4: 186–194

[12] Jawaid M and Khalil H P S A 2011 Cellulosic/synthetic fibre reinforced polymer hybrid composites: a review. *Carbohyd. Polym*. 86: 1–18

[13] Ahmed K S and Vijayarangan S 2008 Tensile, flexural and interlaminar shear properties of woven jute and jute-glass fabric reinforced polyester composites. *J. Mater. Process. Technol.* 207: 330–335

[14] Flynn J, Amiri A and Ulven C 2016 Hybridized carbon and flax fiber composites for tailored performance. *Mater. Des*. 102: 21–29

[15] Gujjala R, Ojha S and Acharya S K 2014 Mechanical properties of woven jute-glass hybrid reinforced epoxy composite. *J. Compos. Mater*. 48: 3445–3455

[16] Rafiquzzaman M, Islam M M and Rahman M H 2016 Mechanical property evaluation of glass–jute fiber reinforced polymer composites. *Polym. Adv. Technol*. 27: 1308–1316

[17] Elbaky M A A 2017 Evaluation of mechanical properties of jute/glass/carbon fibers reinforced hybrid composites. *Fib. Polym*. 18: 2417–2432

[18] Sezgin H and Berkalp O B 2016 The effect of hybridization on significant characteristics of jute/glass and jute/carbon-reinforced composites. *J. Ind. Text*. 47: 283–296

[19] Nayak SK, Mohanty S and Samal S K 2009 Influence of short bamboo/glass fiber on the thermal, dynamic mechanical and rheological properties of polypropylene hybrid composites. *Mater. Sci. Eng. A*. 523: 32–38

[20] Jarukumjorn K and Suppakarn N 2009 Effect of glass fiber hybridization on properties of sisal fiber-polypropylene composites. *Compos. Part B: Eng*. 40: 623–627

[21] Atiqah A, Jawaid M, Sapuan S and Ishak M 2019 Dynamic mechanical properties of sugar palm/glass fiber reinforced thermoplastic polyurethane hybrid composites. *Polym. Compos*. 40: 1329–1334

[22] Margabandu S and Subramaniam S 2019 Experimental evaluation and numerical validation of bending and impact behaviours of hybrid composites with various stacking arrangements. *Mater. Res. Exp*. https://doi.org/10.1088/20531591/ab54e7

[23] Sathishkumar G K, Rajkumar G Srinivasan K and Umapathy M J 2018 Structural analysis and mechanical properties of lignite fly-ash-added jute-epoxy polymer matrix composite. *J. Reinf. Plast. Compos.* 37: 90–104

[24] Jauhari N, Mishra R and Thakur H 2015 Natural fiber reinforced composite laminates - a review. *Mater. Today: Proce*. 2: 2868–2877

[25] Mir A, Zitoune R and Collombet F 2010 study of mechanical and thermomechanical properties of jute/epoxy composite laminate. *J. Reinf. Plast. Compos*. 29: 1669–1680

[26] Goliath A, Kumar M S, Elayaperumal A 2014 Experimental investigations on mechanical properties of jute fibre reinforced composites with polyester and epoxy resin matrices. *Proce. Eng*. 97: 2052–2063

[27] Zin M H, Abdan K, Mazlan N, Zainudin E S and Liew K E 2018 The effects of alkali treatment on the mechanical and chemical properties of pineapple leaf fibres (PALF) and adhesion to epoxy resin. IOP Conference Series: *Mater. Sci. Eng*. 368: 012035

[28] Kabir M M, Wang H, Aravinthan T, Cardona F and Lau K T 2011 Effects of Natural Fibre Surface on Composite Properties: A Review. In: *Proceedings of the 1st international postgraduate conference on engineering, designing and developing the built environment for sustainable well-being (eddBE2011),* 94–99

[29] Ray D, Das M and Mitra D 2009 Influence of alkali treatment on creep properties and crystalinity of jute fibres. *BioResources*, 4: 730–739

[30] Vinayagamoorthy R and Rajeswari N 2014 Mechanical performance studies on vetiveria zizanioides/jute/glass fiber-reinforced hybrid polymeric composites. *J. Reinf. Plast. Compos.* 33: 81–92

[31] Ramamoorthy S K, Di Q, Adekunle K and Skrifvars M 2012 Effect of water absorption on mechanical properties of soyabean oil thermosets reinforced with natural fibers. *J. Reinf. Plast. Compos.* 31: 1191–1200

[32] Suthenthiraveerappa V and Gopalan V 2017 Elastic constants of tapered laminated woven jute/epoxy and woven aloe/epoxy composites under the influence of porosity. *J. Reinf. Plast. Compos.* 36: 1453–1469

[33] Munoz E and García-Manrique, J A 2015. Water absorption behaviour and its effect on the mechanical properties of flax fibre reinforced bio epoxy composites. *Int. J. Polym. Sci*. https://doi.org/10.1155/2015/390275

[34] Pinto M A, Chalivendra V B, Kim Y K and Lewis A F 2014 Evaluation of surface treatment and fabrication methods for jute fiber/epoxy laminar composites. *Polym. Compos.* 35: 310–317

[35] Kumar R, Kumar K, Bhowmik S and Sarkhel G 2019 Tailoring the performance of bamboo filler reinforced epoxy composite: insights into fracture properties and fracture mechanism. *J. Polym. Res.* 26: https://doi.org/10.1007/s10965-019-1720-x

[36] Athijayamani A, Thiruchitrambalam M, Natarajan U and Pazhanivel B 2012 Effect of moisture absorption on the mechanical properties of randomly oriented natural fibers/polyester hybrid composite. *Mater. Sci. Eng. A*. 517: 344–353

[37] Aji I S, Zainudin E S, Abdan K, Sapuan S M and Khairul M D 2012 Mechanical properties and water absorption behavior of hybridized kenaf/pineapple leaf fibre-reinforced high-density polyethylene composite. *J. Compos. Mater*. 47: 979–990

[38] Naveen J, Jawaid M, Zainudin E S, Sultan M T H and Yahaya R 2019 Mechanical and moisture diffusion behaviour of hybrid Kevlar/cocos nucifera sheath reinforced epoxy composites. *J. Mater. Res. Technol*. 8: 1308–1318

[39] Sanjay M A and Yogesha B 2016 Studies on mechanical properties of jute/E-glass fiber reinforced epoxy hybrid composites. *J. Min. Mater. Charac. Eng*. 4: 15–25

[40] Ramesh M, Logesh R, Manikandan M, Kumar N S and Pratap D V 2017 Mechanical and water intake properties of banana-carbon hybrid fiber reinforced polymer composites. *Mater. Res*. 20: 365–376

[41] Murugan R, Ramesh R, Padmanabhan K, Jeyaraam R and Krishna S 2014 Experimental investigation on static mechanical properties of glass/carbon hybrid woven fabric composite laminates. *Adv. Mater. Res*. 903: 96–101

[42] Arthanarieswaran V P, Kumaravel A and Kathirselvam M 2014 Evaluation of mechanical properties of banana and sisal fibre reinforced epoxy composites: Influence of glass fibre hybridization. *Mater. Des.* 64: 194–202

[43] Dhakal H N, Zhang Z Y, Guthrie R, MacMullen J and Bennett N 2013 Development of flax/carbon fibre hybrid composites for enhanced properties. *Carbohyd. Polym*. 96: 1–8

[44] Ramnath B V, Kokan S J, Raja R N, Sathyanarayanan R, Elanchezhian C, Prasad A R and Manickavasagam V M 2013 Evaluation of mechanical properties of abaca-jute-glass fibre reinforced epoxy composite. *Mater. Des*. 51: 357–366

[45] Arumugam S, Kandasamy J, Md Shah A U, Hameed Sultan M T, Safri S N A, Abdul Majid M S, Basri A A and Mustapha F 2020 Investigations on the Mechanical Properties of Glass Fiber/Sisal Fiber/Chitosan Reinforced Hybrid Polymer Sandwich Composite Scaffolds for Bone Fracture Fixation Applications. *Polym.* 12: 1501

[46] Ma H and Joo CW 2010 Structure and mechanical properties of jute–polylactic acid biodegradable composites. *J. Compos. Mater*. 45: 1451–1460

[47] Alemdar A and Sain M 2008 Biocomposites from wheat straw nanofibers: morphology, thermal and mechanical properties. *Compos. Sci. Technol*. 68: 557–565

[48] Padal K T B, Ramji K and Prasad V V S 2014 Mechanical properties of jute nanofibres reinforced composites. *Glo. J. Res. Eng*. 14: 1–6

[49] Tshboi M 1957 Infrared spectrum and crystal structure of cellulose. *J. Polym. sci*. 25: 159–171

[50] Jabasingh S A and Nachiyar C V 2012 Process optimization for the biopolishing of jute fibers with cellulases from Aspergillus Nidulans AJ SU04. *Int. J.Biosci., Biochem. Bioinfor*. 2: 12–15

[51] Sreekumar P A, Leblanc N, Saiah R, Joseph K, Unnikrishnan G and Thomas S 2008 Thermal behavior of chemically treated and untreated sisal fiber reinforced composites fabricated by resin transfer molding. *Compos. Int*. 15: 629–650

[52] Arunavathi S, Eithiraj R D, and Veluraja K 2017 Physical and mechanical properties of jute fiber and jute fiber reinforced paper bag with tamarind seed gum as a binder: An eco-friendly material. *AIP Conf. Proc*. 1832: https://doi.org/10.1063/1.4980228

[53] Sinha E and Rout S K 2009 Influence of fibre-surface treatment on structural, thermal and mechanical properties of jute fibre and its composite. *Bull. Mater. Sci*. 32: 65–76

[54] Amantes B P, Melo R P, Neto R P C and Marques M F V 2017 Chemical treatment and modification of jute fiber surface. *Chem. Chem. Technol*. 11: 333–343

[55] Kabir M M, Islam M M and Wang H 2013 Mechanical and thermal properties of jute fiber reinforced composites. *J. Multi. Compos*. 1: 71–77